Modeling dense pyroclastic basal flows from collapsing columns

E. E. Doyle,[1] A. J. Hogg,[2] H. M. Mader,[1] and R. S. J. Sparks[1]

Received 6 November 2007; revised 10 January 2008; accepted 18 January 2008; published 26 February 2008.

[1] A two layer model for the formation of dense pyroclastic basal flows from dilute, collapsing volcanic eruption columns is presented. The collapsing dilute current is described by depth averaged, isothermal, continuum conservation equations. The dense basal flow is modelled as a granular avalanche of constant density. Simulations demonstrate that pyroclastic flow formation and behavior is dependent upon slope conditions when the dilute part of the current has lost most of its mass. The dilute current runout increases with decreasing particle size and increasing initial column height. If the dilute current has transferred its mass to the dense basal flow on volcanic slopes with inclination angle greater than the friction angle of the basal flow, then the basal flow will continue to propagate until frictional forces bring it to rest. If the dilute current terminates on lower angled slopes, frictional forces dominate the basal flow preventing further front propagation. **Citation:** Doyle, E. E., A. J. Hogg, H. M. Mader, and R. S. J. Sparks (2008), Modeling dense pyroclastic basal flows from collapsing columns, *Geophys. Res. Lett.*, *35*, L04305, doi:10.1029/2007GL032585.

1. Introduction

[2] Pyroclastic density currents are generated by the collapse of explosive eruption columns [*Sparks and Wilson*, 1976], by collapse of lava domes [*Cole et al.*, 2002] and by secondary processes when dilute ash clouds interact with topography [*Druitt et al.*, 2002]. Here a pyroclastic flow is defined as the dense basal part of a pyroclastic density current, characterized by high particle concentration, while a dilute current is defined as the pyroclastic surge component [*Druitt*, 1998]. Transformations between the dense and dilute components of pyroclastic density currents are fundamental to the formation and propagation of dense basal pyroclastic flows [*Fisher*, 1979]. In column collapses, an initially dilute current generates a dense basal flow, and secondary pyroclastic flows can be generated from the ash-cloud surges which originate from block-and-ash flows.

[3] Pyroclastic density currents are generally modeled as either a dilute turbulent suspension [e.g., *Sparks et al.*, 1978; *Neri and Macedonio*, 1996] or a dense pyroclastic flow, such as those produced from dome collapses [e.g., *Wadge et al.*, 1998]. The dilute suspension approach is appropriate for simulations of the initial stages of a column collapse and for the behavior of ash-cloud surges. However, the dilute cloud assumption cannot accurately describe particle accumulation in the basal regions of pyroclastic currents. In addition, the numerics often require a large vertical mesh resolution which prevents an accurate description of any basal flow formation [*Neri et al.*, 2007]. To understand flow transformations, numerical models must couple the dense and dilute regions of these currents and incorporate the interactions between them. *Takahashi and Tsujimoto* [2000] developed a model for the formation of upper surge clouds from dome collapse block-and-ash flows. *Naaim and Gurer* [1998] have developed a similar model in the context of snow avalanches. Here a two layer model for the formation of dense pyroclastic flows from dilute currents is developed.

2. Numerical Model

[4] A collapsing volcanic eruption column generates a dilute particle suspension current, of thickness H, from which a dense basal flow develops (Figure 1). Particles are suspended in the incompressible gas phase and the particulate mixture is treated as a continuum. Effects of diffusion and entrainment on particle concentration are neglected. Turbulent mixing is assumed to preserve a vertically uniform particle concentration, with no loss of the fluid phase [*Bonnecaze et al.*, 1993]. Entrainment of ambient air is neglected because buoyancy is conserved under mixing [*Hallworth et al.*, 1996] and has little effect on the initial dynamics. The dilute current propagates into an ambient of density ρ_a, along a slope inclined at θ to the horizontal (where x is parallel to the slope and z perpendicular, Figure 1). An isothermal average cloud temperature of 850 K is assumed. Heat transfer to the ground and with entrained air is not considered. The interstitial ideal gas phase has a representative density of ρ_g = 0.61 kg/m^3, assuming a pressure P of 0.15 MPa [*Sparks et al.*, 1997].

[5] For the dilute current, the bulk density is defined $\beta = \rho_s\phi + (1-\phi)\rho_g$ for a volumetric concentration ϕ of solid particles with a density ρ_s. The well-mixed particles of diameter d settle from the base at a high Reynolds terminal velocity [*Sparks et al.*, 1997]:

$$\omega = \left(\frac{4\left(\rho_s - \rho_g\right)gd}{3C_d\rho_g}\right)^{1/2} \quad (1)$$

where g is the gravity and the drag coefficient C_d is herein set to 1 [*Woods and Bursik*, 1991]. Depth averaging leads to the conservation of bulk mass equation:

$$\frac{\partial(\beta H)}{\partial t} + \frac{\partial(\beta H u)}{\partial x} = -\omega\rho_s\phi \quad (2)$$

[1]Centre for Environmental and Geophysical Flows, Department of Earth Sciences, University of Bristol, Bristol, UK.

[2]Centre for Environmental and Geophysical Flows, School of Mathematics, University of Bristol, Bristol, UK.

0094-8276/08/2007GL032585$05.00

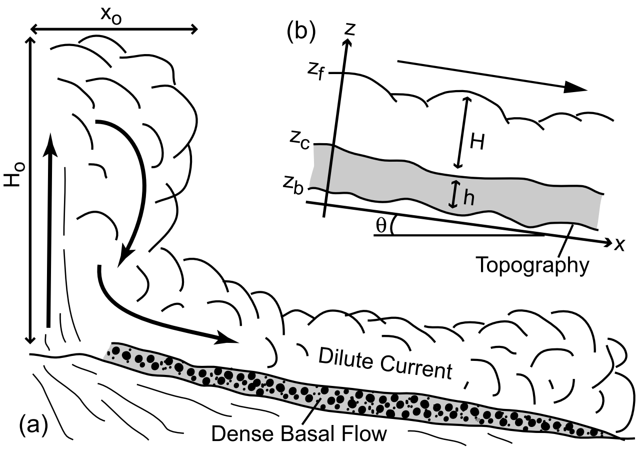

Figure 1. Schematic of the coupled pyroclastic flow model. (a) A typical eruption column collapse is represented by the release from rest of a constant volume of height H_o and width x_o. (b) This generates a dilute ash suspension current of thickness H, propagating along a slope inclined at θ to the horizontal, with x parallel to the slope and z perpendicular. Sedimentation from this turbulent cloud forms a dense basal flow of thickness h.

and the conservation of bulk momentum:

$$\frac{\partial(\beta H u)}{\partial t}+\frac{\partial(\beta H u^2+(\beta-\rho_a)g\cos\theta H^2/2)}{\partial x} = (\beta-\rho_a)gH\sin\theta+(\rho_a-\beta)g\cos\theta H\frac{\partial z_c}{\partial x} - \omega\rho_s\phi u-\beta C_D(u-u_b)|u-u_b| \quad (3)$$

where u defines the depth averaged velocity, z_f is the free surface and z_c the basal contact of the dilute current (Figure 1). The interface drag is parameterized analogously to a basal drag where C_D = 0.001 [*Hogg and Pritchard*, 2004], and u_b is the basal flow's depth averaged velocity. Finally, conservation of the gas phase is defined:

$$\frac{\partial H}{\partial t}+\frac{\partial(Hu)}{\partial x}=0. \quad (4)$$

[6] The dense basal flow has a constant bulk density $\beta_b = \rho_s\phi_b + (1-\phi_b)\rho_g$, where the solid and gas densities are the same as the upper dilute current. A bulk concentration of $\phi_b \approx 0.5$ is assumed, consistent with field estimates [*Sparks*, 1976; *Druitt*, 1998]. Depth averaging from the base z_b to the upper contact z_c, leads to the conservation of mass:

$$\frac{\partial h}{\partial t}+\frac{\partial(u_b h)}{\partial x}=\frac{\omega\rho_s\phi}{\beta_b} \quad (5)$$

and the conservation of momentum:

$$\frac{\partial(hu_b)}{\partial t}+\frac{\partial\left(hu_b^2+g\cos\theta h^2/2\right)}{\partial x} = gh\sin\theta-\frac{\tau_b}{\beta_b}-g\cos\theta h\frac{\partial z_b}{\partial x}+\frac{\omega\rho_s\phi u_b}{\beta_b} \quad (6)$$

neglecting the stress at the upper surface z_c [*Takahashi and Tsujimoto*, 2000], by assuming it is negligible relative to the boundary stress τ_b.

[7] This basal flow is treated as a granular material in which emplacement is controlled by a Coulomb friction $\tau_b = \mathrm{sgn}(u_b)\,\beta_b\, g\, h \cos\theta \tan\delta$ at the base z_b, with a dynamic basal friction angle δ [*Pouliquen*, 1999]. If granular materials are gas fluidized, their dynamic friction can be greatly reduced [*Roche et al.*, 2004]. *Freundt* [1999] estimates the internal granular friction angle to be in the range of 10–30° for small volume and 1° for large volume pyroclastic flows. For simulations herein, a dynamic friction of δ = 10° is chosen as a typical value for small dense flows, noting that such flows typically start to deposit on slopes of 10°–6°.

3. Numerical Method

[8] For both layers, the finite volume method is used to solve the governing equations [*Doyle*, 2007]. The first order upwind Godunov method is adopted and, for the basal flow (equations 5 and 6), the standard shallow-water Roe solver is used to calculate the flux contributions into each numerical cell [*Leveque*, 2002]. Source terms are then calculated via a fractional step approach. The topographic term of equation (6) is included via the flux difference splitting method of *Hubbard and Garcia-Navarro* [2000]. For the dilute current (equations 2–4), the alternative 'f-wave' approach [*Bale et al.*, 2003] is used instead of the Roe solver, already incorporating the topographic terms.

[9] Following standard practice, a stationary negligible prelayer of thickness $\epsilon = 10^{-8}$ m is applied throughout the domain to prevent non-physical solutions when h, or H, is < 0. For the dilute current, this contains a dilute volume concentration of particles ($\phi_a = 10^{-8}$) suspended in the ambient gas ρ_a. Solutions do not depend on these prelayer values. Following standard practice, the dense basal front x_{gf} is determined by the location where the height reduces to a minimum grain size of 100 μm, and the dilute current front $x_{\beta f}$ where the bulk density equals that in the prelayer $\beta_a(\phi_a)$.

[10] The dense basal flow is validated against the shallow water analytical solution [*Shen and Meyer*, 1963; *Mangeney et al.*, 2000]. When Δx = 5 m, the numerical method captures the flow shape with differences of < 5% at the thin flow front [*Doyle*, 2007]. For both models, inclusion of the topography terms is successfully validated against test cases [*Hubbard and Garcia-Navarro*, 2000], demonstrating a corresponding difference of < 6% for the ash cloud flow front. Runout distances differ by < 0.5% for grids of 2 or 5 m. Simulations with initial columns of $H_o \leq 1100$ m use 2 m cells, simulations with taller columns use 5 m cells. Simulations of the dilute current continue until the average bulk density $\overline{\beta}$, along its length, reaches an imposed limit. This is chosen to be within 10% of the ambient density β_a, which has a volumetric particle concentration of only $\phi_a = 10^{-8}$. Remaining particles are assumed to either loft in an associated plume or settle into the upper fine ash layers observed in deposits.

4. Initial Simulations

[11] Simulations were conducted over a representative volcanic cone topography, involving a 13° slope for 10 km surrounded by a 1° plateau in a 25 km domain. Initial conditions consider a constant volumetric concentration of

Table 1. Particle Sizes d, Solids Densities ρ_s, Initial Bulk Densities of the Eruptive Bulk Mixture β_o, and Calculated Particle Settling Velocities ω Used for Simulations[a]

d	ρ_s,	$\beta_o = \rho_s\phi_o + (1 - \phi_o)\rho_g$(kg/m^3)		ω,
-	kg/m^3	(ϕ_o = 0.01)	(ϕ_o = 0.005)	m/s
125 μm	2400	24.6	12.6	2.52
500 μm	2000	20.6	10.6	4.61
1 mm	1750	18.1	9.4	6.1
2 mm	1500	15.6	8.1	8.0
8 mm	1000	10.6	5.6	13.1
16 mm	800	8.6	4.6	16.5
5 cm	800	8.6	4.6	29.2
10 cm	800	8.6	4.6	41.2
50 cm	800	8.6	4.6	92.3

[a]Solids densities are from *Freundt* [1999].

ϕ_o collapsing from rest (Figure 1). Initial column collapse heights H_o of 150, 550, 1100 and 1600 m were considered, inferred from observations of small to medium volume eruptions [*Sparks et al.*, 1997]. The radius of the fully expanded collapsing column x_o is calculated from a typical aspect ratio of $a = H_o/x_o = 3$. Although this aspect ratio is relatively large, we assume that the shallow water model provides an accurate description of the motion after the initial stages of propagation. Particles with diameters from 125 μm to 50 cm are found in most pyroclastic flow deposits [*Walker*, 1971; *Sparks*, 1976], but individual flows vary considerably in grain size from coarse to fine particles. For each column height, simulations are run for each of these different particle sizes at two initial solids volume concentrations ϕ_o = 0.01 and 0.005 (Table 1), assuming that density ρ_s decreases with increasing diameter d [*Freundt*, 1999].

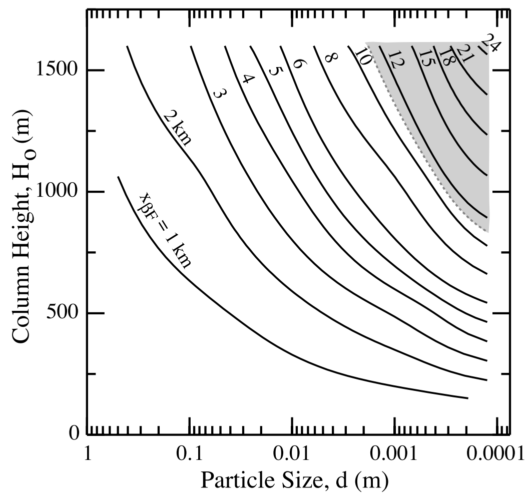

Figure 3. The contoured maximum runout of the dilute part of the current x_{β_F}, with respect to initial column height H_o and particle size d (Table 1) for ϕ_o = 0.01. Dense basal flows propagate beyond the dilute current when the latter terminates on the inclined slope (un-shaded region and Figure 2b). Alternatively, if the dilute current terminates on the low angled plateau then the total propagation is dominated by that of the dilute current (shaded region and Figure 2c). These relationships are also observed for the shorter dilute current runouts produced when ϕ_o = 0.005 and are typical for other geometries.

5. Results

[12] While the dilute part of the current exists, the dense basal flow front x_{gf} is coincident with the dilute current front, $x_{\beta f}$ (Figure 2a). During this phase the density difference between the dilute current and ambient is reduced via sedimentation, but the downslope gravitational acceleration balances this to yield an approximately constant velocity. Currents containing coarser particles show greater deceleration. Once the dilute current has lost its particle load the dense basal flow may continue to propagate independently. Our model demonstrates two types of behavior. First, if the dilute current terminates on a slope with an inclination angle θ exceeding that of the basal friction angle of the dense basal

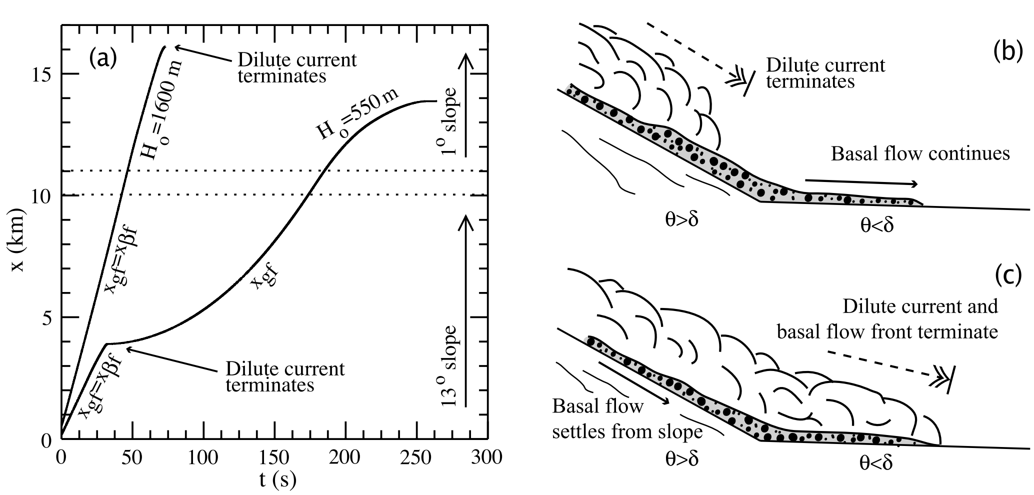

Figure 2. (a) The front position of the dilute current $x_{\beta f}$ and the dense basal flow x_{gf} with respect to time for two initial column collapse heights, H_o = 1600 m and 550 m. Particle size d = 500 μm, basal flow's friction angle δ = 10°. The horizontal lines indicate the gradual change between the 13° slope and 1° plateau. (b) Corresponding schematic of the behavior when the dilute current terminates on the steep slope of angle $\theta > \delta$. (c) Schematic of behavior when the dilute current front terminates on the lower angled plateau, where $\theta < \delta$.

flow δ, then the basal flow continues to move beyond the upper dilute current (Figure 2b), accelerating down slope. The bulk of the thin basal flow initially migrates and thickens towards its front, after which the flow accelerates. Once on the plateau, friction decelerates the flow to rest. The runout increases with decreasing friction angle.

[13] In the second type of behavior, the dilute current terminates on the plateau. Friction dominates the dense basal flow on this plateau, preventing further propagation of its front (Figure 2c). The back of the basal flow may continue to settle from the inclined slopes. The distance from the vent to any slope change, such as the plateau, and the dilute current runout are important parameters controlling simulated basal flow behavior. The maximum dilute current runout increases with increasing column height and decreasing particle size (Figure 3). Increasing the particle size decreases the total sedimentation time to less than the time it takes for the current to reach the plateau, resulting in independent propagation of the basal flow.

6. Discussion

[14] Conceptual models, based upon observations of grain size and density within deposits, identify end member currents as dilute turbulent pyroclastic surges or dense pyroclastic flows [e.g., *Sparks*, 1976; *Druitt*, 1998]. However, there is still debate as to whether there is a distinct boundary between these flow types or whether they represent the extremes of a continuum of possible behaviors. In one end member, mass rapidly transfers from the dilute collapsing eruption column to form a basal flow, propagating as a concentrated suspension for much of its travel distance [e.g., *Sparks*, 1976; *Wilson*, 1985]. Alternatively, if mass transfer is slow, the bulk of material is transported in a dilute turbulent suspension for most of the flow time [e.g., *Dade and Huppert*, 1996].

[15] Both end members are physically plausible within the framework of the simplified two layer model presented here. Coarse grains and low column heights are characterized by rapid mass transfer from the initial dilute suspension to the dense basal pyroclastic flow, with the dense flow significantly out-running the original dilute cloud. This behavior has been observed for column collapses at Montserrat and Lascar [*Druitt et al.*, 2002; *Calder et al.*, 2000].

[16] Fine ash clouds may continue to be generated from dense basal pyroclastic flows by shear [*Denlinger*, 1987], or fluidization [*Calder et al.*, 1997], but such clouds contain little of the mass and are distinct in origin from the original collapsing dilute column. The model also helps in the understanding of facies variations in pyroclastic flow deposits. Lag breccias commonly delineate the region in which collapsing columns transform into dense pyroclastic flows [*Druitt and Sparks*, 1982; *Calder et al.*, 2000], which then extend several times further. The Soncor and 1993 pumice flow deposits at Lascar are examples of this behavior [*Calder et al.*, 2000].

[17] There are several caveats implicit to the results of such a simplified model. Our model is only in the depositional regime. Including air entrainment may reduce sedimentation and thus increase the dilute current runout. The drag from the dilute current on the upper surface of the basal flow and associated entrainment have not been included. High velocity currents and those on steep slopes can be erosive. The model also assumes sedimented particles accumulate to form a propagating basal flow controlled by dynamic friction, and not a direct deposit. With these caveats, the simulations show that modeling of the dense basal flow is usually essential to capture the maximum potential run-out of these hazardous flows.

[18] **Acknowledgments.** EED was supported by a UK Natural Environment Research Council PhD grant NER/S/A/2003/11201. The research of RSJS is supported by a Royal Society Wolfson Research Merit Award.

References

Bale, D. S., R. J. Leveque, and J. A. Rossmanith (2003), A wave propagation method for conservation laws and balance laws with spatially-varying flux functions, *SIAM J. Sci. Comput.*, *24*, 955–978.

Bonnecaze, R., H. Huppert, and J. Lister (1993), Particle-driven gravity currents, *J. Fluid Mech.*, *250*, 339–369.

Calder, E. S., R. S. J. Sparks, and A. W. Woods (1997), Dynamics of co-ignimbrite plumes generated from pyroclastic flows of Mount St. Helens (7 August 1980), *Bull. Volcanol.*, *58*(6), 432–440.

Calder, E. S., R. S. J. Sparks, and M. Gardeweg (2000), Erosion, transport and segregation of pumice and lithic clasts in pyroclastic flows inferred from ignimbrite at Lascar Volcano, Chile, *J. Volcanol. Geotherm. Res.*, *104*, 201–235.

Cole, P. D., E. S. Calder, R. S. J. Sparks, A. B. Clarke, T. H. Druitt, S. R. Young, R. A. Herd, C. L. Harford, and G. E. Norton (2002), Deposits from dome-collapse and fountain-collapse pyroclastic flows at Soufrière Hills Volcano, Montserrat, *Geol. Soc. Mem.*, *21*, 231–262.

Dade, W. B., and H. E. Huppert (1996), Emplacement of the Taupo ignimbrite by a dilute turbulent flow, *Nature*, *381*, 509–512.

Denlinger, R. P. (1987), A model for generation of ash clouds by pyroclastic flows, with application to the 1980 eruptions at Mount St. Helens, Washington, *J. Geophys. Res.*, *92*(B10), 10,284–10,298.

Doyle, E. E. (2007), Analogue and numerical modelling of gravity currents and pyroclastic flows, Ph.D. thesis, Dep. of Earth Sci., Univ. of Bristol, Bristol, U. K.

Druitt, T. H. (1998), Pyroclastic density currents, in *The Physics of Explosive Volcanic Eruptions*, *Geol. Soc. Spec. Publ.*, vol. 145, edited by J. Gilbert and R. Sparks, pp. 145–182, Geol. Soc., London.

Druitt, T., and R. S. J. Sparks (1982), A proximal ignimbrite breccia facies on Santorini, Greece, *J. Volcanol. Geotherm. Res.*, *13*, 147–171.

Druitt, T. H., E. S. Calder, P. D. Cole, R. P. Hoblitt, S. C. Loughlin, G. E. Norton, L. J. Ritchie, R. S. J. Sparks, and B. Voight (2002), Small-volume, highly mobile pyroclastic flows formed by rapid sedimentation from pyroclastic surges at Soufrière Hills Volcano, Montserrat: An important volcanic hazard, *Geol. Soc. Mem.*, *21*, 263–279.

Fisher, R. (1979), Models for pyroclastic surges and pyroclastic flows, *J. Volcanol. Geotherm. Res.*, *6*, 305–318.

Freundt, A. (1999), Formation of high grade ignimbrites. Part II: A pyroclastic suspension current model with implications also for low-grade ignimbrites, *Bull. Volcanol.*, *60*, 545–567.

Hallworth, M. A., H. E. Huppert, J. C. Phillips, and R. S. J. Sparks (1996), Entrainment into two-dimensional and axisymetric gravity currents, *J. Fluid Mech.*, *308*, 289–311.

Hogg, A. J., and D. Pritchard (2004), The effects of hydraulic resistance on dam-break and other shallow inertial flows, *J. Fluid Mech.*, *501*, 179–212.

Hubbard, M. E., and P. Garcia-Navarro (2000), Flux difference splitting and the balancing of source terms and flux gradients, *J. Comput. Phys.*, *165*, 89–125.

Leveque, R. J. (2002), *Finite Volume Methods for Hyperbolic Problems*, Cambridge Univ. Press, Cambridge, U. K.

Mangeney, A., P. Heinrich, and R. Roche (2000), Analytical solution for testing debris avalanche and numerical models, *Pure Appl. Geophys.*, *157*, 1081–1096.

Naaim, M., and I. Gurer (1998), Two-phase numerical model of powder avalanche: Theory and application, *Nat. Hazards*, *117*, 129–145.

Neri, A., and G. Macedonio (1996), Numerical simulation of collapsing volcanic columns with particles of two sizes, *J. Geophys. Res.*, *101*(B4), 8153–8174.

Neri, A., T. Esposti Ongaro, G. Menconi, M. De'Michieli Vitturi, C. Cavazzoni, G. Erbacci, and P. J. Baxter (2007), 4D simulation of explosive eruption dynamics at Vesuvius, *Geophys. Res. Lett.*, *34*, L04309, doi:10.1029/2006GL028597.

Pouliquen, O. (1999), Scaling laws in granular flows down rough inclined planes, *Phys. Fluids*, *11*(3), 542–548.

Roche, O., M. A. Gilbertson, J. C. Phillips, and R. S. J. Sparks (2004), Experimental study of gas-fluidized granular flows with implications for pyroclastic flow emplacement, *J. Geophys. Res.*, *109*, B10201, doi:10.1029/2003JB002916.

Shen, M. C., and R. Meyer (1963), Climb of a bore on a beach. Part 3: Run-up, *J. Fluid Mech.*, *16*, 113–125.

Sparks, R. S. J. (1976), Grain size variations in ignimbrites and implications for the transport of pyroclastic flows, *Sedimentology*, *23*, 147–188.

Sparks, R. S. J., and L. Wilson (1976), A model for the formation of ignimbrite by gravitational column collapse, *J. Geol. Soc. London*, *132*, 441–451.

Sparks, R. S. J., L. Wilson, and G. Hulme (1978), Theoretical modeling of the generation, movement and emplacement of pyroclastic flows by column collapse, *J. Geophys. Res.*, *83*(B4), 1727–1739.

Sparks, R., M. Bursik, S. Carey, J. Gilbert, L. Glaze, H. Sigurdsson, and A. Woods (1997), Pyroclastic flows, in *Volcanic Plumes*, chap. 6, pp. 141–179, John Wiley, Hoboken, N. J.

Takahashi, T., and H. Tsujimoto (2000), A mechanical model for Merapi-type pyroclastic flow, *J. Volcanol. Geotherm. Res.*, *98*, 91–115.

Wadge, G., P. Jackson, and S. M. Bower (1998), Computer simulations of pyroclastic flows from dome collapse, *Geophys. Res. Lett.*, *25*(19), 3677–3680.

Walker, G. P. L. (1971), Grain size characteristics of pyroclastic deposits, *J. Geol.*, *79*, 696–714.

Wilson, C. (1985), The Taupo eruption, New Zealand. Part II: The Taupo ignimbrite, *Philos. Trans. R. Soc. London, Ser. A.*, *314*, 229–310.

Woods, A. W., and M. I. Bursik (1991), Particle fallout thermal disequilibrium and volcanic plumes, *Bull. Volcanol.*, *53*, 559–570.

E. E. Doyle, H. M. Mader, and R. S. J. Sparks, Centre for Environmental and Geophysical Flows, Department of Earth Sciences, University of Bristol, Wills Memorial Building, Queen's Road, Bristol BS8 1RJ, UK. (emmadoyle79@gmail.com)

A. J. Hogg, Centre for Environmental and Geophysical Flows, School of Mathematics, University of Bristol, University Walk, Bristol BS8 1TW, UK.